PROCEEDINGS OF SCIENCE

Gamma ray astronomy with ARGO-YBJ

Tristano Di Girolamo[*†]
Università "Federico II" and INFN, Napoli, Italy
E-mail: tristano@na.infn.it

The ARGO-YBJ air shower detector has been in stable data taking for five years at the YangBaJing Cosmic Ray Laboratory (Tibet, P.R. China, 4300 m a.s.l.) with a duty cycle $> 86\%$ and an energy threshold of a few hundreds of GeV. With the scaler mode technique, the minimum threshold of 1 GeV can be reached. In this paper the latest results in gamma ray astronomy will be presented, including those of the observation, in scaler mode, of 206 Gamma Ray Bursts, the largest sample ever investigated with a ground-based detector at high energies.

Science with the New Generation of High Energy Gamma-ray experiments, 10th Workshop
04-06 June 2014
Lisbon - Portugal

[*]Speaker.
[†]On behalf of the ARGO-YBJ collaboration.

PoS(Scineghe2014)039

1. The detector

The ARGO−YBJ experiment is located at Yangbajing (Tibet, P.R. China, 4300 m a.s.l.) and consists of a single layer of Resistive Plate Counters (RPCs) on a total area of about 110×100 m^2. The detector has a modular structure, the basic module being a cluster (5.7×7.6 m^2), made of 12 RPCs. Each RPC is divided into 10 pads, whose data acquisition (DAQ) is independent and which represent the time pixels of the detector (55.6×61.8 cm^2). The digital readout of each pad is made by means of 8 strips, which are the space pixels (6.75×61.8 cm^2) [1]. The detector carpet is connected to two different DAQ systems, which work independently: in shower mode, for each event the location and timing of each detected particle is recorded, allowing the reconstruction of the lateral distribution and of the arrival direction; in scaler mode, the counting rate of each cluster is measured every 0.5 s, with little information on the space distribution and arrival direction of the detected particles. The trigger of the shower mode was $N_{pad} \geq 20$ in a time window of 420 ns, with a rate 3.5 kHz. In the scaler mode DAQ, for each cluster four scalers record the rate of counts ≥ 1, ≥ 2, ≥ 3 and ≥ 4 in a time window of 150 ns. The corresponding measured rates are, respectively, $\sim$40 kHz, $\sim$2 kHz, $\sim$300 Hz and $\sim$120 Hz [2]. The experiment has been taking data with its full layout from November 2007 to February 2013.

The detector pointing accuracy, angular resolution and absolute energy calibration have been determined studying the deficit in the cosmic ray flux due to the Moon. In particular, the opening angle ψ_{70}, containing 71.5% of the cosmic ray events from a point source, is about 2° for $N_{pad} \geq 20$, 1.36° for $N_{pad} \geq 60$ and 1.0° for $N_{pad} \geq 100$, while an improvement of $\sim 30-40\%$ is expected for gamma-induced showers because of their better defined time profile [3].

2. Sky survey

The ARGO-YBJ detector surveyed the northern hemisphere, in the declination band from -10° to 70°, at energies above 0.3 TeV. With an integrated sensitivity down to 0.24 Crab unit[1] (depending on the declination) after five years of data taking, six sources were detected with a statistical significance S$>$ 5 standard deviations (s.d.), and five excesses are reported as potential (S$>$ 4 s.d.) gamma ray emitters [4]. The list of excess regions, with their corresponding significances for $N_{pad} \geq 20$ (except ARGO J1841-0332, for which $N_{pad} \geq 100$) estimated with equation (9) of [5] and corresponding TeV associations, is given in Table 1.

In the following, a selection of results concerning the sources detected in the sky survey will be presented.

2.1 Crab Nebula

The angular distributions of the events around the Crab Nebula position are in agreement with the point spread functions obtained by Monte Carlo simulations. The differential energy spectrum obtained for this source in the range 0.3-20 TeV can be described by the power law $dN/dE = (5.2 \pm 0.2) \times 10^{-12} (E/2\ TeV)^{(-2.63 \pm 0.05)}$ photons cm^{-2} s^{-1} TeV^{-1}, which gives an integral flux above 1 TeV of 1.97×10^{-11} photons cm^{-2} s^{-1}. Figure 1 shows this spectrum compared with results from other experiments [6].

[1]The Crab unit here is defined as the integral flux 3.30×10^{-11} photons cm^{-2} s^{-1} above $\sim$0.7 TeV

ARGO-YBJ Name	Significance (s.d.)	TeV Association
ARGO J0409-0627	4.8	
ARGO J0535+2203	20.8	Crab Nebula
ARGO J1105+3821	14.1	Mrk 421
ARGO J1654+3945	9.4	Mrk 501
ARGO J1839-0627	6.0	HESS J1841-055
ARGO J1907+0627	5.3	HESS J1908+063
ARGO J1910+0720	4.3	
ARGO J1912+1026	4.2	HESS J1912+101
ARGO J2021+4038	4.3	VER J2019+407
ARGO J2031+4157	6.1	MGRO J2031+41
		TeV J2032+4130
ARGO J1841-0332	4.2	HESS J1843-033

Table 1: List of ARGO-YBJ excess regions with corresponding statistical significances and TeV associations. All significances are given for $N_{pad} \geq 20$ except that of ARGO J1841-0332, which is for $N_{pad} \geq 100$.

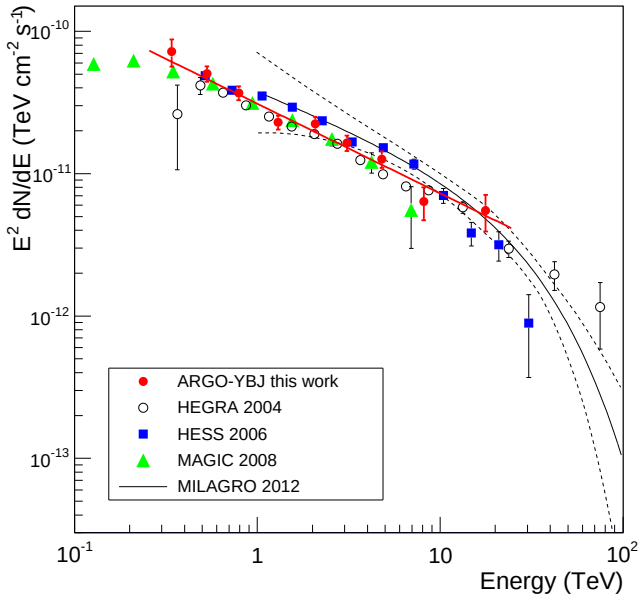

Figure 1: Crab Nebula differential energy spectrum multiplied by E^2 as measured by ARGO-YBJ and other experiments. The straight solid line represents the best fir of the ARGO-YBJ data, while the dotted lines delimitate the 1σ error band of the Milagro spectrum.

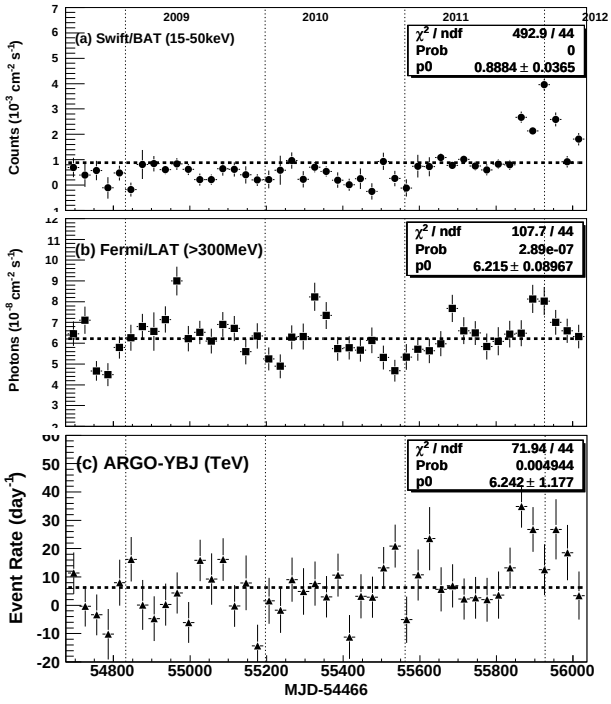

Figure 2: Light curves of Mrk 501 as measured by Swift/BAT, Fermi/LAT and ARGO-YBJ. Each bin contains 30 days, the vertical bars represent 1σ uncertainties, the horizontal dashed lines show the constant values resulting from fits.

With data collected in five years of observations, the distribution of the daily excesses from the Crab Nebula for events with $N_{pad} \geq 40$ gives an average counting rate of (137 ± 10) day^{-1} and can be fitted by a Gaussian function with mean value -0.04 ± 0.03 and r.m.s.=1.05 ± 0.02.

2.2 Mrk 501

During its five years of operation, ARGO-YBJ monitored Mrk 501 at energies above 0.3 TeV [7]. The largest flare was observed from October 2011 to April 2012, with the brightest episode from October 17 to November 22, when the excess of the event rate reached 6.1 s.d., corresponding to $\sim$2 Crab units above 1 TeV, which means an increase to a flux 6.6 ± 2.2 larger than the long-term steady one. The measured light curve, compared with those observed by Swift/BAT in the 15-150 keV range and by Fermi/LAT above 0.3 GeV, is given in Figure 2. During the X-ray flare at the end of 2011 (Swift/BAT flux enhanced by a factor $\sim$4) it is evident the increase of the TeV flux, while the GeV flux does not rise significantly.

ARGO-YBJ detected emission above 8 TeV with a significance larger than 4σ, which did not happen since the Mrk 501 flare in 1997 [8]. Considering the spectral energy distribution, a simple one-zone synchrotron self-Compton model fits well the long-term data, however is unable to reproduce the flaring emission at energies $>$8 TeV due to the hardness of the spectrum.

A monitoring and study of flaring emission was carried out by ARGO-YBJ also for Mrk 421 [9].

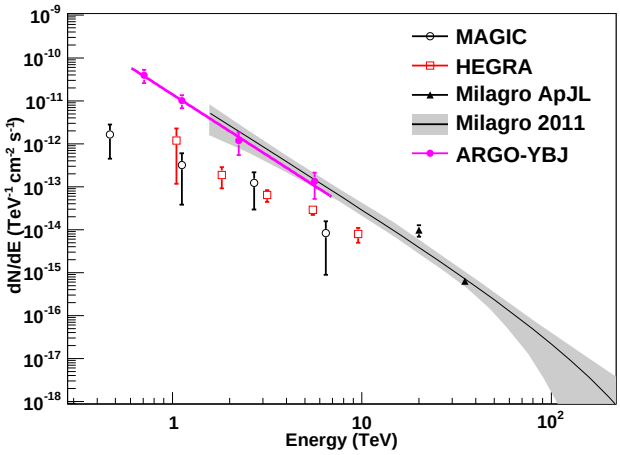

Figure 3: Spectrum of MGRO J2031+41 as measured by ARGO-YBJ and other experiments.

2.3 Extended sources: the Cygnus region

The Cygnus region is the brightest portion of the gamma ray northern sky, where several complex structures have been observed at different wavelengths. This region is rich in potential cosmic ray acceleration sites, including Wolf-Rayet stars, OB associations, supernova remnants and pulsars. Various Very High Energy (VHE) gamma ray sources have been detected within the Cygnus region, the brightest being the extended MGRO J2031+41/TeV J2032+4130 and MGRO J2019+37 [10], whose locations are consistent with two Fermi pulsars [11].

ARGO-YBJ detected a signal with a significance larger than 6 s.d. at the position of MGRO J2031+41 [12]. The source extension is determined to be $\sigma_{ext} = (0.2^{+0.4}_{-0.2})^\circ$, consistent with the previous estimations by HEGRA [13] and MAGIC [14] experiments, i.e., $\sigma_{ext} = 0.103^\circ \pm 0.025^\circ$ and $\sigma_{ext} = 0.083^\circ \pm 0.030^\circ$, respectively. Assuming an intrinsic extension $\sigma_{ext} = 0.1^\circ$, the energy spectrum measured in the range 0.6-7 TeV is $dN/dE = (1.40 \pm 0.34) \times 10^{-11} (E/1\,TeV)^{(-2.83 \pm 0.37)}$ photons cm^{-2} s^{-1} TeV^{-1} and is reported in Figure 3. The integral flux above 1 TeV is $\sim$0.3 Crab unit, in agreement with Milagro results [15, 16] but about a factor 10 higher than the fluxes determined by HEGRA and MAGIC.

In a location consistent with MGRO J2031+41, Fermi/LAT detected a complex extended source, attributed to the emission by a "cocoon" of freshly accelerated cosmic rays which fill the cavities carved by stellar winds and ionization fronts from young stellar clusters [17]. After re-analysing the complete ARGO-YBJ data set, subtracting the contribution of the overlapping TeV sources and using a larger region to evaluate the excess map (since Fermi/LAT observations revealed a large extended source), ARGO J2031+4157 resulted with an extension $\sigma_{ext} = 1.8^\circ \pm 0.5^\circ$, consistent with that of the Cygnus Cocoon as measured by Fermi/LAT, i.e., $\sigma_{ext} = 2.0^\circ \pm 0.2^\circ$ [18]. The ARGO-YBJ view of the Cygnus Cocoon region (for $N_{pad} \geq 20$) is given in Figure 4, where the largest statistical significance is 6.1 s.d., at the position of ARGO J2031+4157.

The spectrum also shows a good connection with that determined by Fermi/LAT in the 1-100 GeV energy range, as shown in Figure 5. Therefore, ARGO J2031+4157 is identified as the counterpart of the Cygnus Cocoon at TeV energies. The combined differential spectrum of

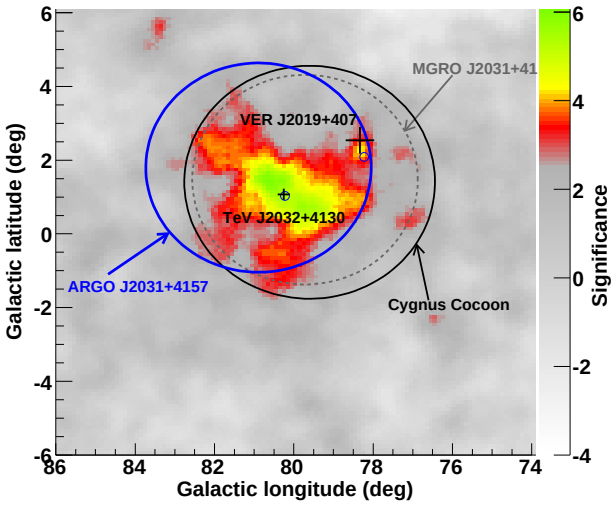

Figure 4: Significance map around ARGO J2031+4157 as observed by ARGO-YBJ. The large circles indicate the positions and 68% contours of ARGO J2031+4157, MGRO J2031+41 and the Cygnus Cocoon. The positions and extensions of TeV J2032+4130 [13] and VER J2019+407 [19] are marked with crosses.

Fermi/LAT and ARGO-YBJ data is fitted with the power law function $dN/dE = (3.5 \pm 0.3) \times 10^{-9}(E/0.1\ TeV)^{(-2.16\pm0.04)}$ photons cm^{-2} s^{-1} TeV^{-1} (dot-dashed line in Figure 5).

In order to reproduce the gamma ray emission from the Cygnus Cocoon, a purely hadronic model [20] can be adopted, in which the observed gamma rays are due to the decay of π^0 mesons resulting from inelastic collisions between accelerated protons and target gas. Assuming that the primary proton spectrum follows a power law with exponential cutoff, the maximum cutoff energy allowed by the ARGO-YBJ highest energy upper limit is E_c=150 TeV (solid line in Figure 5). Taking into account also the Milagro data, E_c would be around 40 TeV (dotted line).

Concerning MGRO J2019+37, which is the second brightest source after the Crab Nebula with Milagro data at $\sim$12 TeV, having an extension $\sigma_{ext} = 0.32^\circ \pm 0.12^\circ$ [21], the ARGO-YBJ map does not show any excess above 3 s.d., and flux upper limits were set at 90% confidence level (c.l.) [12]. Recently, the VERITAS observatory imaged MGRO J2019+37, spatially resolving it into two different sources: the faint point-like VER J2016+371 and the bright extended ($\sim 1^\circ$) VER J2019+368, which likely contributes to the bulk of the emission observed by Milagro and is positionally coincident with the pulsar PSR J2021+3651 and the star formation HII region Sh 2-104 [22]. All these results are reported in Figure 6.

Considering also the ARGO-YBJ results for MGRO J1908+06 [23] and HESS J1841-055 [24], as for the Milagro air shower array, the fluxes measured in extended sources are systematically larger than those measured with Cherenkov telescopes. The origin of this discrepancy, which is not present for point-like sources, is not clear. For ARGO-YBJ, the overall systematic error on the flux measurements has been estimated to be $< 30\%$ [25]. There could be some systematic effect related to the methods for background evaluation of the different experimental techniques [24].

Moreover, a contribution is expected from the diffuse gamma ray emission produced by the interaction of cosmic rays with matter in the Galactic plane, however, according to ARGO-YBJ

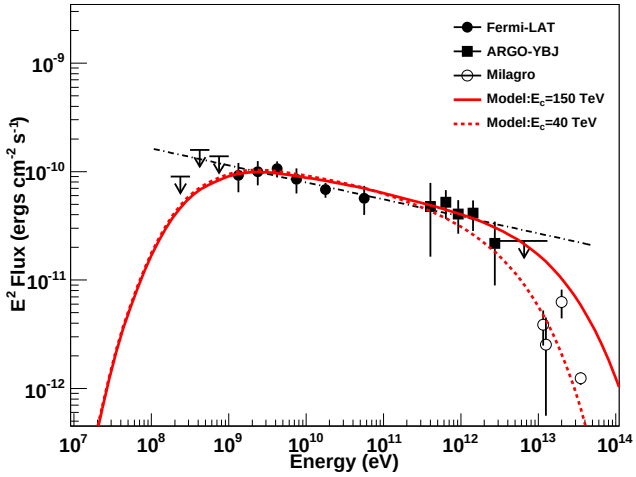

Figure 5: Spectrum of the Cygnus Cocoon as measured by different detectors. The arrows below 1 GeV indicate the upper limits set by Fermi/LAT, the Milagro data refer to MGRO J2031+41, at 12 TeV corrected for the extrapolation of TeV J2032+4130 [17]. The dot-dashed line shows the power law best fit to the combined Fermi/LAT and ARGO-YBJ data. The solid and dotted curves are predicted by a purely hadronic model with proton cutoff energy at 150 TeV and 40 TeV, respectively.

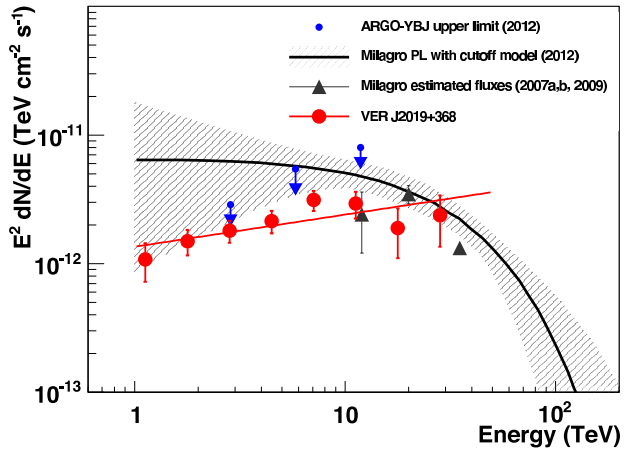

Figure 6: Observational results for MGRO J2019+37 from different experiments. The Milagro power law with cutoff best fit, with its 1σ error band (shadowed area), is taken from [16].

measurements, it is different for each extended source but always less than 15% of the detected flux [26].

3. Search for Gamma Ray Bursts in scaler mode

In scaler mode, the energy threshold for photons is about 1 GeV, lower than the highest energies detected by satellite experiments. Moreover, the modular structure of the ARGO-YBJ detector allowed the collection of data during the different mounting phases. Therefore a search for emis-

sion from Gamma Ray Bursts (GRBs) in coincidence with satellite detections started in November 2004, when the Swift satellite was launched [27]. Until February 2013 a sample of 206 GRBs was analysed, 24 of them with known redshift z. This is the largest sample of GRBs investigated with a ground-based detector at high energies. Since no significant signal was found in the data, the fluence upper limits in the 1-100 GeV energy range were determined at 99% c.l. assuming two different power law spectra: a) the index measured by satellite detectors in the keV-MeV energy range; b) the conservative differential index -2.5. For case a), when double power law spectral features have been identified, the higher spectral index (i.e., that above the peak in the keV-MeV region of the $E^2 \cdot dN/dE$ spectrum) has been used. For the set of 24 GRBs with known redshift the ranges of upper limits between the values corresponding to the two spectral assumptions are represented by rectangles in Figure 7, while a simple arrow is shown if the low energy spectrum is a cutoff power law, and thus only case b) is considered. For GRB090902B (which was the GRB in the ARGO-YBJ field of view with the highest photon energy detected) the fluence extrapolated from Fermi-LAT observations in the same energy range is shown [28]. Only for this GRB the GeV spectral index measured by Fermi-LAT was used and the dashed area in Figure 7 was obtained with a maximum energy of the GRB spectrum ranging from 30 GeV (about the maximum energy measured by Fermi-LAT) to 100 GeV. Moreover, an upper limit on the GRB cutoff energy E_{cut} can be set by the intersection of the fluence upper limit, as a function of E_{cut}, with the extrapolation to the interval 1 GeV-E_{cut} of the fluence measured by satellites. Figure 8 reports the E_{cut} upper limits for the 30 GRBs for which the intersection occurs in the 2-100 GeV range, as a function of the differential spectral index. For GRBs with unknown redshift, z=2 and z=0.6 were assumed for long and short classes, respectively. More results and details about this search can be found in [29].

References

[1] G. Aielli et al., *Layout and performance of the RPCs used in the ARGO-YBJ experiment*, *NIM A* **562** 92 (2006)

[2] G. Aielli et al., *Scaler Mode Technique for the ARGO-YBJ detector*, *Astropart. Phys.* **30** 85 (2008)

[3] B. Bartoli et al., *Observation of the cosmic ray Moon shadowing effect with the ARGO-YBJ experiment*, *PRD* **84** 022003 (2011)

[4] B. Bartoli et al., *TeV gamma ray survey of the northern sky using the ARGO-YBJ detector*, *ApJ* **779** 27 (2013)

[5] T. P. Li & Y. Q. Ma, *Analysis methods for results in gamma-ray astronomy*, *ApJ* **272** 317 (1983)

[6] B. Bartoli et al., *Crab Nebula: five-year observation with ARGO-YBJ*, *ApJ* in press (2014)

[7] B. Bartoli et al., *Long-term monitoring of Mrk 501 for its very high energy γ emission and a flare in 2011 October*, *ApJ* **758** 2 (2012)

[8] M. Amenomori et al., *Detection of multi-TeV gamma rays from Markarian 501 during an unforeseen flaring state in 1997 with the Tibet Air Shower Array*, *ApJ* **532** 302 (2000)

[9] B. Bartoli et al., *Long-term monitoring of the TeV emission from Mrk 421 with the ARGO-YBJ experiment*, *ApJ* **734** 110 (2011)

[10] A. A. Abdo et al., *TeV gamma-ray sources from a survey of the Galactic Plane with Milagro*, *ApJ* **664** L91 (2007)

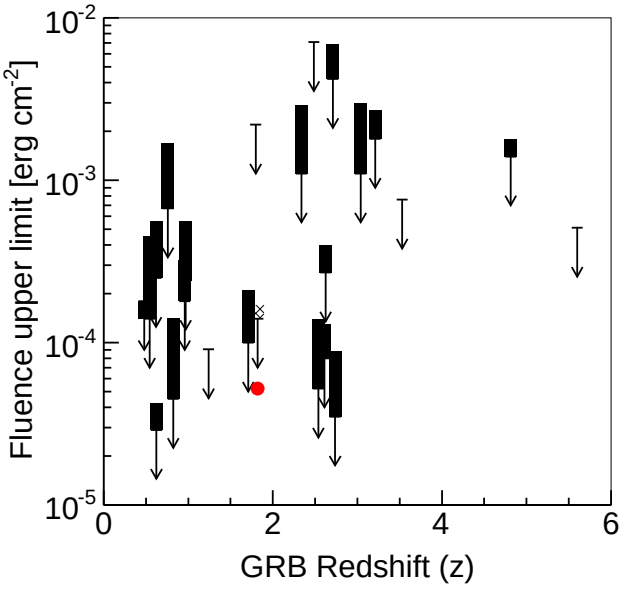

Figure 7: Fluence upper limits in the 1-100 GeV energy range for the 24 GRBs with known redshift, obtained with differential spectral indexes ranging from the value measured by satellites to -2.5 (only this latter case is considered for cutoff power law spectra). The dot shows the fluence extrapolated in the 1-100 GeV interval from the Fermi-LAT observations of GRB090902B (see text for its upper limit determination).

[11] P. L. Nolan et al., *Fermi Large Area Telescope Second Source Catalog*, *ApJS* **199** 31 (2012)

[12] B. Bartoli et al., *Observation of TeV gamma rays from the Cygnus region with the ARGO-YBJ experiment*, *ApJ* **745** L22 (2012)

[13] F. Aharonian et al., *The unidentified TeV source (TeV J2032+4130) and surrounding field: Final HEGRA IACT-System results*, *A&A* **431** 197 (2005)

[14] J. Albert et al., *MAGIC observations of the unidentified gamma ray source TeV J2032+4130*, *ApJ* **675** L25 (2008)

[15] A. A. Abdo et al., *Milagro observations of multi-TeV emission from Galactic sources in the Fermi Bright Source List*, *ApJ* **700** L127 (2009)

[16] A. A. Abdo et al., *Spectrum and morphology of the two brightest Milagro sources in the Cygnus region: MGRO J2019+37 and MGRO J2031+41*, *ApJ* **753** 159 (2012)

[17] M. Ackermann et al., *A Cocoon of Freshly Accelareted Cosmic Rays Detected by Fermi in the Cygnus Superbubble*, *Science* **334** 1103 (2011)

[18] B. Bartoli et al., *Identification of the TeV gamma-ray source ARGO J2031+4157 with the Cygnus Cocoon*, *ApJ* **790** 152 (2014)

[19] E. Aliu et al., *Discovery of TeV gamma-ray emission toward Supernova Remnant SNR G78.2+2.1*, *ApJ* **770** 93 (2013)

[20] L. O'C. Drury, F. Aharonian & H. J. Völk, *The gamma-ray visibility of supernova remnants. A test of cosmic ray origin*, *A&A* **287** 959 (1994)

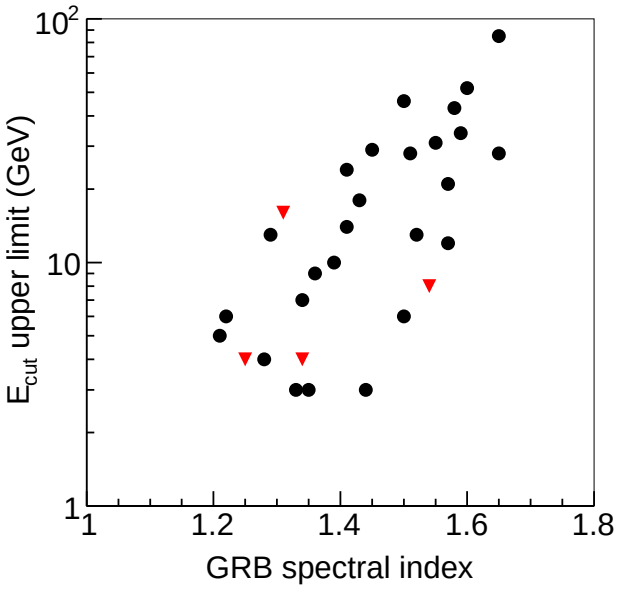

Figure 8: Cutoff energy upper limits as a function of the differential spectral index obtained by extrapolating the measured keV-MeV spectra. The values represented by triangles are obtained taking into account the extragalactic absorption at the known GRB redshift, for the others z=2 and z=0.6 are assumed for long and short classes, respectively.

[21] A. A. Abdo et al., *Discovery of TeV gamma-ray emission from the Cygnus region of the Galaxy*, *ApJ* **658** L33 (2007)

[22] E. Aliu et al., *Spatially resolving the very high energy emission from MGRO J2019+37 with VERITAS*, *ApJ* **788** 78 (2014)

[23] B. Bartoli et al., *Observation of the TeV gamma ray source MGRO J1908+06 with ARGO-YBJ*, *ApJ* **760** 110 (2012)

[24] B. Bartoli et al., *Observation of TeV gamma rays from the unidentified source HESS J1841-055 with the ARGO-YBJ experiment*, *ApJ* **767** 99 (2013)

[25] G. Aielli et al., *Gamma ray flares from Mrk 421 in 2008 observed with the ARGO-YBJ detector*, *ApJ* **714** L208 (2010)

[26] B. Bartoli et al., *Study of the diffuse gamma-ray emission from the Galactic plane with ARGO-YBJ*, in preparation

[27] G. Aielli et al., *Search for Gamma Ray Bursts with the ARGO-YBJ detector in scaler mode*, *ApJ* **699** 1281 (2009)

[28] A. A. Abdo et al., *Fermi observations of GRB 090902B: a distinct spectral component in the prompt and delayed emission*, *ApJ* **706** L138 (2009)

[29] B. Bartoli et al., *Search for GeV Gamma Ray Bursts with the ARGO-YBJ detector: summary of eight years of observations*, *ApJ* in press (2014)